Calcium Phosphate Nanocomposite Particles for *In Vitro* Imaging and Encapsulated Chemotherapeutic Drug Delivery to Cancer Cells

Mark Kester[1], **Y. Heakal**[1], **A. Sharma**[1], **Gavin P. Robertson**[1], **Thomas T. Morgan**[2], **Erhan İ Altinoğlu**[2], **Amra Tabaković**[2], **Mylisa R. Parette**[2], **Sarah Rouse**[2], **Victor Ruiz-Velasco**[1], and **James H. Adair**[2],*

[1]Penn State College of Medicine, 500 University Drive, Hershey, Pennsylvania 17033

[2]Material Science and Engineering Department, The Pennsylvania State University, 249 Materials Research Labs Hastings Road University Park, Pennsylvania 16802

Abstract

Paradigm-shifting modalities to more efficiently deliver drugs to cancerous lesions require the following attributes: nanoscale-size, targetability and stability under physiological conditions. Often, these nanoscale drug delivery vehicles are limited due to agglomeration, poor solubility or cytotoxicity. Thus, we have designed a methodology to encapsulate hydrophobic antineoplastic chemotherapeutics within a 20-30 nm diameter, pH-responsive, non-agglomerating, non-toxic calcium phosphate nanoparticle matrix. In the present study, we report on calcium phosphate nanocomposite particles (CPNP) that encapsulate both fluorophores and chemotherapeutics, are colloidally stable in physiological solution for extended time at 37°C and can efficaciously deliver hydrophobic antineoplastic agents, such as ceramide, in several cell model systems.

Keywords

Calcium phosphate; nanoparticles; ceramide; *in vitro* chemotherapy; cancer

Nanoparticles with fluorescent properties have been prepared by several synthetic approaches,[1-7] some of which exploit the benefits of self-assembly, particularly reverse micelles, to prepare a wide range of nanocolloids.[8-18] For example, reverse micelle techniques have been used to produce nearly monodisperse fluorescent semiconductor quantum dots with various shapes and sizes as well as to capture organic fluorophores within silica inorganic matrices.[2-6, 19, 20] While suitable for drug delivery *in vitro* where immune responses do not exist, semi-conductor or silica nanocomposite particles with surface decoration are not particularly efficacious for drug delivery in humans.[1, 6, 21] Biodegradation of the decorated therapeutics prior to delivery can be severe. To overcome these limitations and realize the full potential of nanocomposite drug and fluorophore delivery systems, we have developed non-agglomerating nano-sized calcium phosphate-based composite particles. Reasonably high, but benign, concentrations of calcium and phosphate (1 to 5mM) occur in all vertebrates and are naturally non-toxic as well as bioresorbable.[22-24] Calcium phosphate has been widely used to provide transfection of DNA and deliver drugs via surface decoration of calcium phosphate microparticles.[2, 5, 13, 14, 16, 25] The present study reports the colloidal properties of stable, non-aggregating, 20 nm nanocomposite calcium phosphate particles embedded with fluoroprobes and a small

jha3@psu.edu.

amphiphilic neoplastic drug, ceramide, for simultaneous bioimaging and drug delivery to a range of cell types, including melanoma and breast adenocarcinoma cell lines.

One advantage of calcium phosphate as an embedding material relative, for example, to polymeric nanoparticles or liposomes,[25-29] is its variable solubility in cells.[2, 5, 13, 14, 25, 30-32] Many chemotherapeutics cannot be used clinically due to insolubility, phase separation, and toxicology.[25, 29] Therefore, encapsulation of insoluble therapeutics in a pH tunable soluble nanoparticle can provide a novel means of transportation to specific cells or tissues and also optimize their biological concentration at the targeted sites.[2, 5] An example of such a water-insoluble therapeutic molecule is ceramide (Cer), an experimental therapeutic agent which has been shown to play an important role in the apoptosis of cancer cells.[33] Cer is a lipid-derived second messenger[34, 35] that preferentially induces tumor apoptosis[28] by inhibiting over-expressed pro-survival AKT3, a kinase that is activated in 70% of melanomas through AKT3 amplification or PTEN loss.[36] It has been previously shown that as the degree of malignancy increases, the level of Cer in the cell decreases.[37] Despite Cer's potential usefulness as an anti-cancer agent, many of these lipophilic agents, especially those with longer chains, are almost completely insoluble in water, making administration difficult even in several model systems. Currently, in pre-clinical studies, ceramides are either dissolved in dimethylsulfoxide (DMSO) or administered via liposomal micelle encapsulation. [28, 26, 27]

Previous reports have described the synthesis strategy for nanocomposite colloids in detail and thus, will only be briefly described.[7, 8, 18, 19] We have adapted the double reverse-micelle strategy to synthesize amine, carboxylate-, and polyethylene glycol surface functionalized CPNP (See Supporting Information).[7] We utilized the positively charged, amine-functionalized CPNP in all of the following studies. These nanocolloids are routinely composed of 20 nm diameter calcium phosphate particles, with a zeta potential of +30mV. The HPLC concentration strategy yields 10^{15} particles per ml of solution, and removes amphiphile and cyclohexane byproducts to final concentrations of less than 0.5mM and 15ppm, respectively. HPLC-concentrated CPNP remains dispersed for extended time in phosphate buffered saline (PBS), 10mM phosphate buffered at pH 7.4, 0.14M NaCl, and 0.01M KCl, solutions. Using this formulation, CPNP have been introduced into a variety of cell culture media including those that have fetal bovine serum present.

The colloidal stability of some nanocolloids, particularly organic-based systems such as liposomes and dendrimers, can be sensitive to temperature changes because of entropic effects.[11, 38] The colloidal stability of CPNP based on particle size distribution was evaluated in PBS at 37 °C for an extended time by quasi-elastic light scattering (QELS) (Figure 1). The CPNP used for Figure 1 yielded the mean diameter and lognormal standard deviation of 31.30 ± 0.19 nm after 48 hour equilibration at 37°C. This remained relatively unchanged after 288 hours (37.40 nm ± 0.16). The particle size distributions do not significantly change with time up to 288 hours verifying colloidal stability of the CPNPs in physiological solutions and temperature. These data indicate that our approach to preparing CPNP formulations represents a highly stable nanocomposite colloid in physiological conditions for a minimum of two weeks. Our synthetic scheme offers control and design of colloid size distribution, a persistent issue in nanoparticle synthesis.[7, 39]

A unique feature of CPNP is the ability to simultaneously image and deliver therapeutics as a function of solution pH. Calcium phosphates, regardless of Ca:P ratio, crystallinity, or phase, are relatively insoluble at physiological pH (pH 7.4) and become increasingly soluble below pH 6.5.[12-14, 29, 30, 32] We are exploiting this pH tunable solubility to deliver drugs with extreme hydrophobicity, such as ceramide (Cer_6 and Cer_{10}). Despite the efficacy of exogenous Cer delivered via DMSO or liposomes in cell culture systems or in animal

models, the use of Cer as a systemic chemotherapeutic is still limited by hydrophobicity or metabolism, traits shared by many amphiphilic therapeutics. Calcium phosphates are by nature hydrophilic. If a hydrophobic drug is encapsulated, CPNP can be used as a pH-dependent vehicle to deliver the immiscible drug through the blood stream to target tissue or cells where the lower intercellular pH then dissolves the calcium phosphate nanoparticle releasing the drug. Recent submitted data demonstrate, using fluorescence correlation spectroscopy, that low pH either *ex situ* or *in vitro* induces dissolution of the CPNPs, releasing encapsulated Cy3-fluorophore.[7] In the first set of experiments, we wanted to examine whether ceramide-doped CPNP could be employed for both simultaneous imaging and drug delivery in cultured melanoma cells.

Cultured UACC 903 melanoma cells were chosen as a model system since they respond to exogenous Cer with increased apoptosis.[26, 28] Thus, we next investigated the use of Cer-doped CPNP for simultaneous imaging and efficacy of inducing death in human melanoma cell lines. Decanoyl-ceramide (Cer_{10}) and fluorophore, rhodamine-WT (Rh-WT), were encapsulated within the calcium phosphate matrix of each particle. In these experiments, we successfully delivered one of the most hydrophobic ceramides, Cer_{10}, a physiological long chain ceramide that heretofore could not be administered in aqueous formulations. Control CPNP containing fluorophore, but not Cer, exhibited a perinuclear or cytosolic imaging profile in melanoma, distinct from the DAPI-stained nuclei (Figure 2A, left). Of significance, the control CPNP did not induce any significant cellular toxicity (Figure 2A, middle and right panel). In contrast, melanoma cells are particularly sensitive to the apoptotic effects of Cer_{10}-calcium phosphate nanoparticles (2×10^{13} particles/mL of 30 nm-diameter particles that deliver a final Cer_{10} concentration of 10μM (Figures 2B and 2C). Cer concentration was determined by HPLC-MS/MS after EDTA-dissolution of the CPNPs. Cell based cytoxicity assays (See Supporting Information) confirmed that the Cer_{10}-CPNP reduced melanoma cell survival to less than 5% at 5 μM (Figure 2C). The limited cytotoxicity associated with empty control CPNP (no ceramide present) at, or above, 2×10^{13} particles/mL is most likely due to the high concentration of amines associated with the surfaces of particles present in the cytosol of the cells. Our results indicate that an optimal concentration for the combination of ceramide and particle number *in vitro* can be achieved.

Consistent with our studies on melanoma cells, Cer–doped CPNP were also found highly effective for inducing apoptosis in breast cancer cell lines (Figure 3, See Supporting information for experimental procedures). In fact, Cer_{10}-doped CPNP were effective in both drug-sensitive (MCF7) (Figure 3A) and drug-resistant (MCF7/ADR, adriamycin resistant) (Figure 3B) breast cancer cell models. MCF7/ADR, currently known as NCI/ADR, is a drug resistant cancer cell phenotype that is well established to overexpress P-glycoprotein. Although, the origin of this cell line is controversial, over the years it has served as a good model to study multidrug resistance in cancer caused by overexpression of P-glycoprotein.[40, 41] This study provides the first demonstration that Cer administration can induce cellular apoptosis in a drug-resistant model of breast cancer. Specifically, 5-fold lower doses of Cer_{10} in calcium phosphate nanocolloidal formulations elicited a 7-fold increase in caspase 3/7 activity (a marker of apoptosis) than Cer_{10}/DMSO formulations. This is particularly exciting since Cer efficacy is often limited by P-glycoprotein multi-drug resistance receptors that metabolize Cer into less toxic metabolites.[42] Thus, Cer-encapsulated CPNP may offer a non-toxic, nano-strategy to treat drug resistant tumors. Again, there is a slight increase in apoptosis, as indicated by increasing caspase 3/7 activity, for the control formulations composed of amine-functionalized CPNP without Cer present. This finding is consistent with the studies on the melanoma cell culture, suggesting that there is an optimal, sub-toxic, threshold dosage of the CPNP for delivery of therapeutics. These *in vitro* breast cancer studies are the proof-of-concept studies that argue for continue investigation of the efficacy, biodistribution and cellular metabolism of Cer-doped CPNPs.

In the last set of experiments a cell culture model was chosen that could be particularly sensitive to exposure to the CPNP. Thus, we next examined whether fluorescent CPNP could be employed as imaging agents of sympathetic neurons, with little or no toxic effects. Acutely isolated adult rat stellate ganglion (SG) neurons were incubated with fluorescein-encapsulated CPNP. Figure 4a shows fluorescence and phase contrast (inset image) images of SG neurons following 4 hr incubation with 8.1ng/μL CPNP at 37°C. Figure 4A shows that most of the neurons internalized the nanoparticles under these conditions. To verify the lack of CPNP-induced toxicity, the modulation of Ca^{2+} currents by nociceptin (1 μM) was also examined. Nociceptin is the endogenous ligand for the opioid receptor-like 1 (ORL1) receptors expressed in SG neurons, and inhibits Ca^{2+} channel currents in a voltage-dependent manner. The superimposed Ca^{2+} current traces evoked every 10 sec with the 'double-pulse' voltage protocol (see Supporting Information) are given for control (Figure 4Bi) and CPNP-treated (Figure 4Bii) SG neurons. The upper trace in Figures 4Bi and 4Bii was obtained with nociceptin present while the lower trace was obtained without nociceptin. Application of nociceptin produced the typical voltage-dependent inhibition of Ca^{2+} currents characterized by kinetic slowing in both groups of cells. No significant differences were observed in the magnitude of nociceptin-mediated Ca^{2+} current inhibition (Figure 4Biii) between the control and CPNP-exposed neurons. These results verify that exposure of SG neurons to CPNP did not lead to any significant changes in modulation of Ca^{2+} channel currents implying little or no change in neuronal function and/or CPNP-induced toxicity following exposure to the nanoparticles.

This report demonstrates that CPNP are colloidally stable for extended times in physiological conditions and can be used to deliver fluorophores and lipophilic drugs for a variety of cell types. The metabolic pathways for Ca^{2+} uptake and membrane transport are not perturbed and do not elicit acute toxicity in neural cells. Thus, CPNP have broad potential applicability as *ex vivo* and *in vivo* imaging agents as well as for drug delivery platforms.[7] Validation of CPNP as highly efficacious, non-toxic, broadly-based, drug delivery platforms has been detailed in this study. The pH changes occurring during endocytosis leads to dissolution of CPNP and subsequent cytosolic or perinuclear release of encapsulated agents.[7] Thus, drugs with little or no solubility in physiological liquids can be delivered using the CPNP approach. Cer therapeutics provides an excellent demonstration of the efficacy of cellular delivery of a hydrophobic bioactive agent via the CPNP.

Despite the fact that 10^{14} amine functionalized CPNP/mL are systemically injected into animal models with minimal acute toxicity (data not shown), we are still concerned about chronic toxicology, especially given increasing cytotoxicity indicated by the MTS and caspase 3/7 assays with increasing particle number concentration for the control formulations. This observation is not unexpected, as for example, Sayes et al[43] found that *in vitro* cytotoxicity of fullerenes was strongly associated with surface functionalization with cytotoxicity greatest for underivatized n-C_{60}, followed by C_3 and $Na^+_{2-3}[C_{60}O_{7-9}(OH)_{12-15}]^{(2-3)-}$, with $C_{60}(OH)_{24}$ having no cytotoxicity up to the solubility limit. Hoshino et al.[44] found that amine-terminated quantum dot formulations gave one of the higher cytotoxicities as a function of surface speciation. However, variations in particle size distribution with surface functionality in Hoshino et al.[44] give ambiguities regarding cytotoxicity as a function of surface groups. Our current studies are evaluating the effect of surface functionality on both cytotoxicity and biodistribution using citrate, PEG, and amine surface functionalization on the CPNPs.

Supplementary Material

Refer to Web version on PubMed Central for supplementary material.

Acknowledgments

Supporting Information

Experimental methods for CPNP preparation, characterization, SG neuron isolation, imaging, and Ca^{2+} current recording, Melanoma cell imaging and cytotoxicity assays, breast adenocarcinoma apoptosis assays.

References

1. Adair, JH.; Kumar, R.; Antolino, N.; Szepesi, CJ.; Kimel, RA.; Rouse, SM. In: Baumard, JF., editor. Colloidal lessons learned for dispersion of nanosize particulate suspensions; Proceedings of the World Academy of Ceramics; Faenza, Italy. Faenza, Italy: Techna Group SrI; 2005. 2005. p. 93-145.

2. Bisht S, Chattopadhyay D, Maitra A. J. Biomedical Nanotechnology. 2006; 2:229–238.

3. Ostafin AE, Siegel M, Wang Q, Mizukami H. Microporous and Mesoporous Materials. 2003; 57:47–55.

4. Ow H, Larson DR, Srivasatava M, Baird BA, Webb WW, Wiesner U. Nano Letters. 2005; 5(1): 113–117. [PubMed: 15792423]

5. Schmidt HT, Kroczynski M, Maddox J, Chen Y, Josephs R, Ostafin AE. Journal of Microencapsulation. 2006; 23(7):769–781. [PubMed: 17123921]

6. Tan W, Wang K, He X, Zhao XJ, Drake T, Wang L, Bagwe RP. Medicinal Research Reviews. 2004; 24(5):621–638. [PubMed: 15224383]

7. Morgan TT, Muddana HS, Altinoglu EI, Rouse SM, Tabakovic A, Tabouillot T, Russin TJ, Butler PJ, Eklund P, Yun JK, Kester M, Adair JH. Nano Letters. 2008

8. Adair JH, Li T, Kido T, Havey K, Moon J, Mecholsky J, Morrone A, Talham DR, Ludwig MH, Wang L. Materials Science & Engineering R-Reports. 1998; 23(4-5):139–242.

9. Arriagada FJ, Osseoasare K. Colloid Chemistry of Silica. 1994; 234:113–128.

10. Arriagada FJ, Osseoasare K. Journal of Colloid and Interface Science. 1995; 170(1):8–17.

11. Hunter, RJ. Zeta Potential in Colloid Science: Theory and Practice. Academic Press; New York, NY: 1981.

12. Lai C, Tang SQ, Wang YJ, Wei K. Materials Letters. 2005; 59(2-3):210–214.

13. Roy I, Mitra S, Maitra A, Mozumdar S. Int. J. Pharmaceutics. 2003; 250:25–33.

14. Maitra A. Expert Rev. Mol. Diagn. 2005; 5(6):893–905. [PubMed: 16255631]

15. Adair JH, Suvaci E. Current Opinion in Colloid and Interface Science. 2000; 5(1-2):160–167.

16. Bisht S, Bhakta G, Mitra S, Maitra A. Int. J. Pharmaceutics. 2005; 288:157–168.

17. Li T, Moon J, Morrone AA, Mecholsky JJ, Adair JH. Langmuir. 1999; 15(13):4328–4334.

18. Wang J, White WB, Adair JH. J Phys Chem B Condens Matter Mater Surf Interfaces Biophys. 2006; 110(10):4679–85. [PubMed: 16526702]

19. Adair, JH.; Kumar, R.; Antolino, N.; Szepesi, CJ.; Kimel, RA.; Rouse, SM. In: Baumard, JF., editor. Colloidal lessons learned for dispersion of nanosize particulate suspensions; Proceedings of the World Academy of Ceramics; Faenza, Italy. Faenza, Italy: Techna Group SrI; 2005. 2005. p. 93-145.

20. Jaiswal JK, Simon SM. Trends in Cell Biology. 2004; 14(9):497–504. [PubMed: 15350978]

21. Yao G, Wang L, Wu Y, Smith J, Xu J, Zhao W, Lee E, Tan W. Anal Bioanal Chem. 2006; 385:518–524. [PubMed: 16715275]

22. Bonucci, E. Calcification in Biological Systems. CRC Press; Boca Raton: 1992. p. 406

23. Coe, FL.; Favus, MJ.; Pak, CYC.; Parks, JH.; Preminger, GM. Kidney Stones: Medical and Surgical Management. Lippincott-Raven Publishers; Philadelphia: 1996. p. 1109

24. Freshney, RI. Culture of Animal Cells: A Manual of Basic Technique. 3rd. Wiley-Liss, Inc.; New York: 1994. p. 486

25. Yih TC, Al-Fandi M. Journal of Cellular Biochemistry. 2006; 97:1184–1190. [PubMed: 16440317]

26. Shabbits JA, Mayer LD. Anticancer Res. 2003; 23(5A):3663–9. [PubMed: 14666662]

27. Shabbits JA, Mayer LD. Biochim Biophys Acta. 2003; 1612(1):98–106. [PubMed: 12729935]

28. Stover TC, Sharma A, Robertson GP, Kester M. Clinical Cancer Research. 2005; 11(9):3465–3474. [PubMed: 15867249]

29. Panyam P, Labhassetwar V. Advanced Drug Delivery Reviews. 2003; 55:329–347. [PubMed: 12628320]

30. Chander S, Fuerstenau DW. Colloids and Surfaces. 1982; 4:101–120.

31. Magne D, Faucheus C, Grimadi G, Daculsi G, Guicheux J. Drug Discovery Today. 2002; 7(17): 928–931.

32. Prakash KH, Kumar R, Ooi CP, Cheang P, Khor KA. Langmuir. 2006; 22:11002–11008. [PubMed: 17154577]

33. Ogretmen B, Hannun YA. Nature Reviews. 2004; 3:604–616.

34. Fox TE, Finnegan CM, Blumenthal R, Kester M. Cell Mol Life Sci. 2006; 63(9):1017–23. [PubMed: 16568241]

35. Bourbon NA, Sandirasegarane L, Kester M. J Biol Chem. 2002; 277(5):3286–92. [PubMed: 11723139]

36. Stahl JM, Sharma A, Cheung M, Zimmerman M, Cheng JQ, Bosenberg MW, Kester M, Sandirasegarane L, Robertson GP. Cancer Res. 2004; 64(19):7002–10. [PubMed: 15466193]

37. Riboni L, Campanella R, Bassi R, Villani R, Gaini SM, Martinelli-Boneschi F, Viani P, Tettamanti G. Glia. 2002; 39:105–113. [PubMed: 12112362]

38. Napper, DH. Polymeric Stabilization of Colloidal Dispersions. Academic Press; New York, NY: 1983.

39. Funk, JE.; Dinger, DR. Predictive Process Control of Crowded Particulate Suspensions: Applied to Ceramic Manufacturing. Kluwer Publishing; Boston, MA: 1994.

40. Liscovitch M, Ravid DA. Cancer Letters. 2007; 245(1-2):350–352. [PubMed: 16504380]

41. Mehta K, Devarajan E, Chen J, Multani A, Pathak S. Journal of the National Cancer Institute. 2002; 94(21)

42. Gouaze-Andersson V, Cabot MC. Biochim Biophys Acta. 2006; 1758(12):2096–2103. [PubMed: 17010304]

43. Sayes CM, Fortner JD, Guo W, Lyon D, Boyd AD, Ausman KD, Tao YJ, Sitharaman B, Wilson LJ, Highes JB, West JL, Colvin VL. Nano Letters. 2004; 4(10):1881–1887.

44. Hoshino A, Fujioka K, Oku T, Suga M, Sasaki Y, Ohta T, Yasuhara M, Suzuki K, Yamamoto K. Nano Letters. 2004; 4(11):2163–2169.
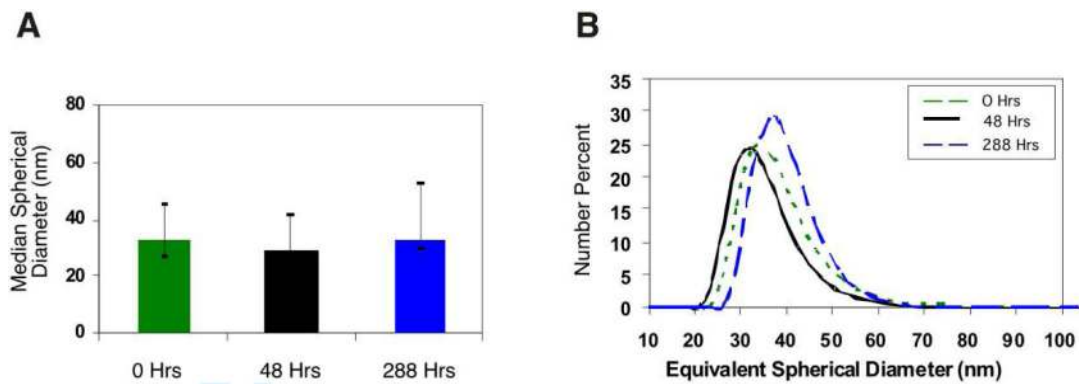
Figure 1.
The hydrodynamic diameter of the CPNPs in PBS was evaluated as a function of time at 37°C to evaluate colloidal stability. (A) Mean hydrodynamic diameter (±standard deviation) for the CPNPs at 0 time, 48 hours, and 288 hours at 37°C and (B) Hydrodynamic diameter distributions for each of the times at physiological temperature.
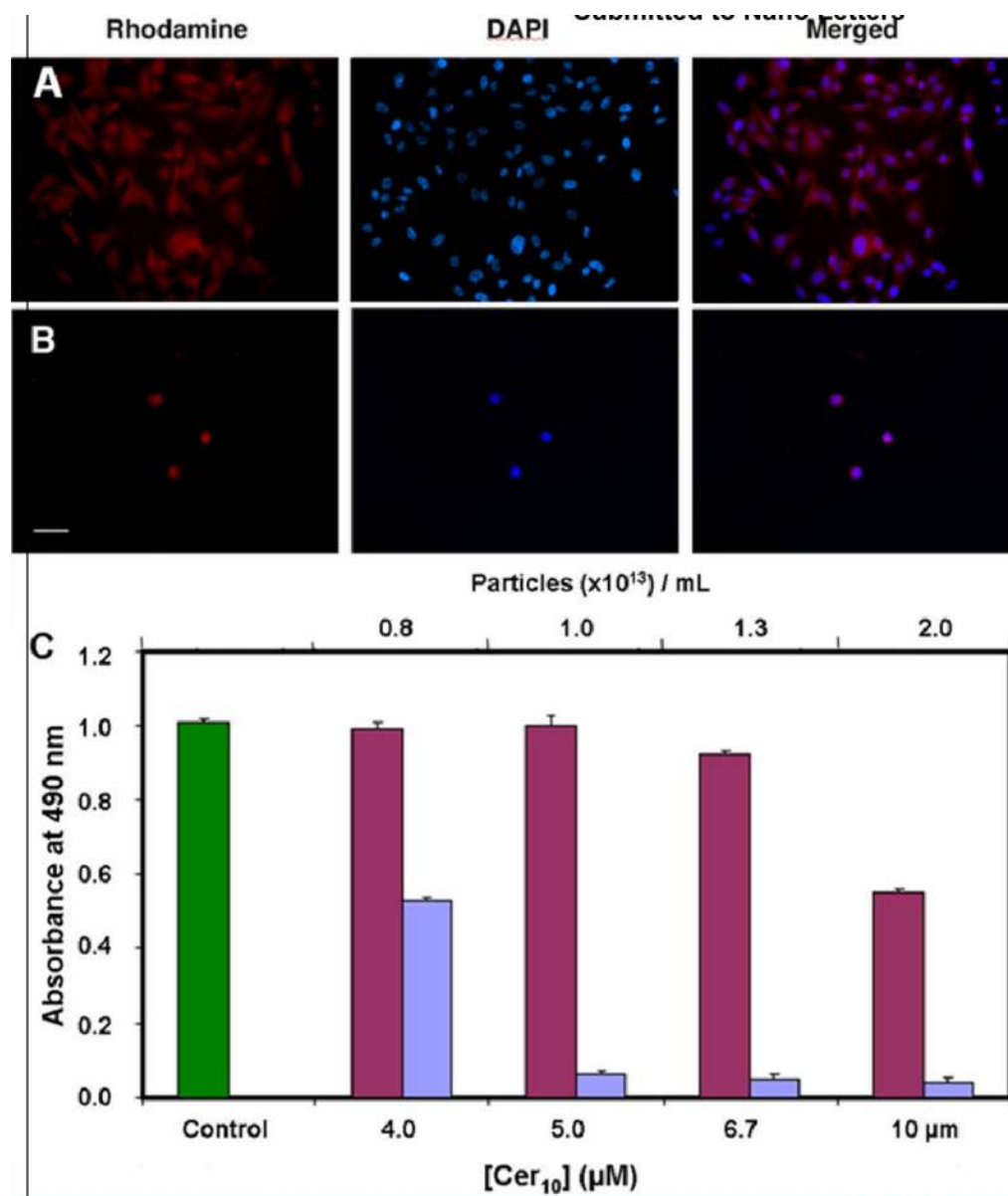
Figure 2. *In vitro* effect of Cer$_{10}$-CPNP on melanoma cell survival and viability
Representative images of cultured melanoma UACC 903 cells exposed to rhodamine WT-CPNP without (**A**) and with (**B**) Cer$_{10}$. Fluorescent Cer$_{10}$-CPNP, unlike control CPNP, induce melanoma cell death; and (**C**) MTS cytotoxicity assay demonstrating dosage responsive cytotoxic actions of Cer$_{10}$-CPNPs. Control CPNPs exhibit modest cytotoxicity at the highest particle number concentration. Values are mean ± SEM for three independent experiments, each experiment replicated in triplicate. The green bar represents Cer$_{10}$ in DMSO, the purple bar represents the CPNP, and the blue bar represents Cer$_{10}$ in CPNP. The scale bars in A and B are 50 μm.
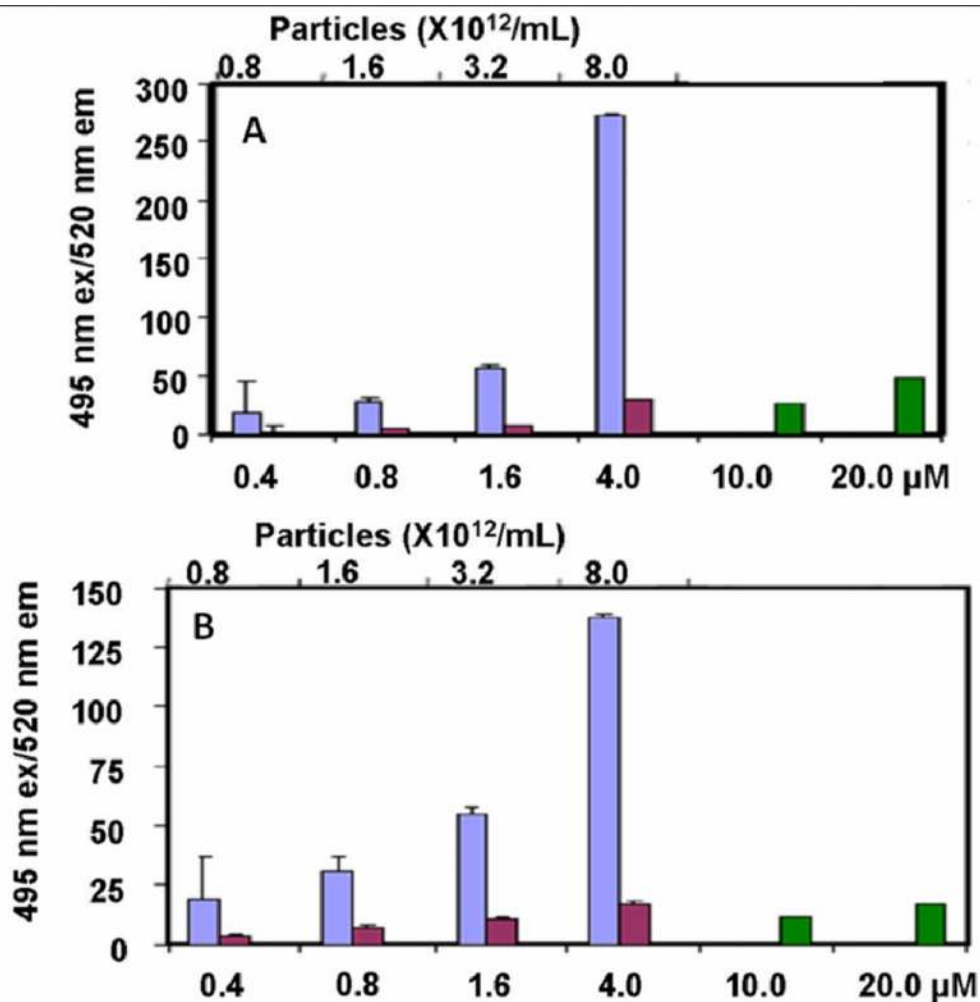
Figure 3.
In vitro apoptotic effects of Cer_{10}-calcium phosphate nanoparticles (CPNPs) on (A) drug sensitive (MCF-7) and (B) drug resistant (MCF-7/ADR) breast adenocarcinoma cell lines. Cer_{10}-CPNPs, but not control CPNPs or Cer_{10} in DMSO, induced robust caspase 3/7 activity, a measure of apoptosis in both drug sensitive and drug resistance cell lines. Values are mean ± SEM for three independent experiments with each experiment replicated in triplicate. ±SEMs for Cer_{10}- CPNPs are too small to be depicted in the graph. The purple bar represents the CPNP while blue and green represent Cer_{10} in CPNP and Cer_{10} in DMSO respectively.
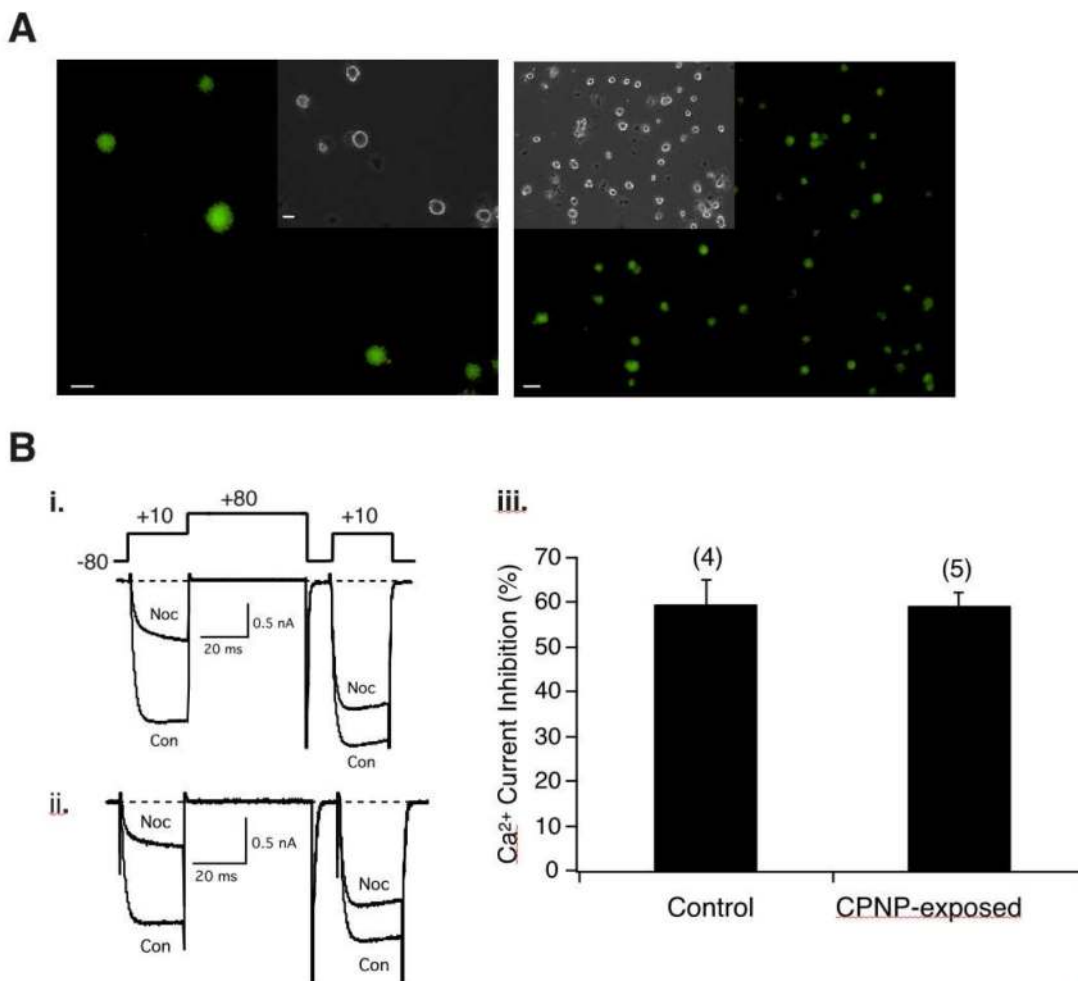
Figure 4.
Uptake of fluorescein-containing CPNP by rat sympathetic stellate ganglion (SG) neurons.
(A) Fluorescence and phase contrast (insets) images of SG neurons following a 4 hr
incubation with fluorescein-encapsulated CPNPs (8.1 ng/μL) at 37°C. SG neurons were
imaged at 10X (right) and 20X (left) and fluorescence images were acquired with a filter set
containing an excitation filter at 480 nm and an emission filter at 535 nm. The fluorescence
images were pseudo-colored; scale bars, 20 μm. (B) i. Superimposed Ca^{2+} current traces
evoked with the 'double-pulse' voltage protocol (shown on top of i) in the absence (lower
trace) or presence (upper trace) of nociceptin (1 μM) for a control (bi) and CPNP-exposed
(ii) neuron. Ca^{2+} currents were evoked every 10 s. (iii) Summary graph of mean (± SEM)
Ca^{2+} current inhibition produced by application of nociceptin in control and neurons
incubated with fluorescein-containing CPNPs (8.1 ng/μL) for 3 hr. Inhibition was
determined from the Ca^{2+} current amplitude measured isochronally at 10 ms into the
prepulse (+10 mV) in the absence or presence of nociceptin. Numbers in parenthesis
indicate the number of experiments.